Afferent and motoneuron activity in response to single neuromast stimulation in the posterior lateral line of larval zebrafish

Melanie Haehnel-Taguchi, Otar Akanyeti and James C. Liao

J Neurophysiol 112:1329-1339, 2014. First published 25 June 2014; doi:10.1152/jn.00274.2014

Journal of Neurophysiology publishes original articles on the function of the nervous system. It is published 12 times a year (monthly) by the American Physiological Society, 9650 Rockville Pike, Bethesda MD 20814-3991. ISSN: 0022-3077, ESSN: 1522-1598. Visit our website at http://www.the-aps.org/.

J Neurophysiol 112: 1329–1339, 2014.
First published June 25, 2014; doi:10.1152/jn.00274.2014.

Afferent and motoneuron activity in response to single neuromast stimulation in the posterior lateral line of larval zebrafish

Melanie Haehnel-Taguchi, Otar Akanyeti, and James C. Liao
The Whitney Laboratory for Marine Bioscience, Department of Biology, University of Florida, Saint Augustine, Florida

Submitted 8 April 2014; accepted in final form 18 June 2014

Haehnel-Taguchi M, Akanyeti O, Liao JC. Afferent and motoneuron activity in response to single neuromast stimulation in the posterior lateral line of larval zebrafish. *J Neurophysiol* 112: 1329–1339, 2014. First published June 25, 2014; doi:10.1152/jn.00274.2014.—The lateral line system of fishes contains mechanosensory receptors along the body surface called neuromasts, which can detect water motion relative to the body. The ability to sense flow informs many behaviors, such as schooling, predator avoidance, and rheotaxis. Here, we developed a new approach to stimulate individual neuromasts while either recording primary sensory afferent neuron activity or swimming motoneuron activity in larval zebrafish (*Danio rerio*). Our results allowed us to characterize the transfer functions between a controlled lateral line stimulus, its representation by primary sensory neurons, and its subsequent behavioral output. When we deflected the cupula of a neuromast with a ramp command, we found that the connected afferent neuron exhibited an adapting response which was proportional in strength to deflection velocity. The maximum spike rate of afferent neurons increased sigmoidally with deflection velocity, with a linear range between 0.1 and 1.0 μm/ms. However, spike rate did not change when the cupula was deflected below 8 μm, regardless of deflection velocity. Our findings also reveal an unexpected sensitivity in the larval lateral line system: stimulation of a single neuromast could elicit a swimming response which increased in reliability with increasing deflection velocities. At high deflection velocities, we observed that lateral line evoked swimming has intermediate values of burst frequency and duty cycle that fall between electrically evoked and spontaneous swimming. An understanding of the sensory capabilities of a single neuromast will help to build a better picture of how stimuli are encoded at the systems level and ultimately translated into behavior.

mechanoreceptor; flow sensing; hair cell deflection; motoneuron; swimming

FISHES DETECT WATER MOTION relative to their bodies with the mechanosensory lateral line system, which in larvae consists of only a few dozen receptors (neuromasts) as opposed to hundreds in adult fishes (Coombs and Janssen 1989; Metcalfe et al. 1985). At the larval stage, all neuromasts lie on the surface of the skin and contain, along with support cells, hair cells of two polarities which are most sensitive to flow from antagonizing directions, along either their anterior-posterior or dorsal-ventral axis (Flock and Wersall 1962). The haircell bundle (stereovilli and kinocilia) of all hair cells in a neuromast project into a gelatinous cupula. Displacement of the cupula shears the hair cell bundle, causing the hair cells to depolarize and increase glutamate release onto afferent neurons, which, in response, generate an increase in action potentials (Dijkgraaf 1963; Trapani and Nicolson 2011).

Address for reprint requests and other correspondence: James C. Liao, The Whitney Laboratory for Marine Bioscience, Dept. of Biology, University of Florida, 9505 OceanShore Blvd., St. Augustine, FL 32080 (e-mail: jliao@whitney.ufl.edu).

The lateral line plays an important role in behaviors as diverse as schooling, predator avoidance, and rheotaxis. This has been demonstrated by comparing the behavioral performance of freely swimming fishes with intact vs. ablated lateral line systems, where a variety of stimuli have been employed, ranging from moving spheres to bulk water flow (Coombes and Conley 1997; McHenry et al. 2009; Montgomery et al. 1997; Olszewski et al. 2012). A more direct understanding of how these stimuli across the body are encoded by the nervous system has been gained with electrophysiological recordings from hair cells (Jielof et al. 1952; Ricci et al. 2013) and from primary afferent neurons in adult fishes (Chagnaud et al. 2008; Engelmann et al. 2000; Kroese and Schellart 1992; Montgomery and Coombs 1992; Voigt et al. 2000). In this study, we also record from afferent neurons. However, to better understand the mechanisms of how flow-related information is encoded by the afferent neurons and how these signals are translated into appropriate motor behaviors, we used larval zebrafish, which have a functional lateral line system and already exhibit a variety of motor behaviors (Budick and O'Malley 2000; Fero et al. 2011; Liao 2010; Liao and Haehnel 2012; Trapani and Nicolson 2011). The transparency and the accessibility to the nervous system in larval zebrafish allow us to record from both peripheral motoneurons, as well as from single afferent neurons that contact identified neuromasts along the body.

The focus of this paper is to better understand sensorimotor integration in the larval lateral line system. We investigate how cupula deflection of a neuromast translates into afferent activity and then motor responses. Specifically, we mechanically deflected the cupula of individual neuromasts using ramp stimulation to test the following. What is the range of deflection amplitudes that elicits a robust afferent response? What is the range of deflection velocities that a neuromast can encode? Is the deflection of the cupula in a single neuromast sufficient to elicit a motor response, and, if so, how much? We believe that an understanding of the sensory capabilities of a single neuromast will help to build a better picture of how stimuli are encoded at the systems level and translated into behavior.

MATERIAL AND METHODS

Animals. Experiments were performed on wild-type zebrafish larvae (*Danio rerio*) at ages 4–6 days postfertilization (dpf) and reared according to standard procedures (Brand et al. 2002). Experiments were performed at room temperature (23–26°C). All procedures were approved by the Institutional Animal Care and Use Committee of the University of Florida.

Lateral line ablation. Larvae were anesthetized with 0.04% tricaine methanesulfonate (Finquel, Argent, Redmont, WA) in 10% Hanks' solution (137 mM NaCl, 5.4 mM KCl, 1 mM $MgSO_4$, 0.44 mM KH_2PO_4, 0.25 mM Na_2HPO_4, 4.2 mM $NaHCO_3$, 1.3 mM $CaCl_2$ for

100% solution, adjusted to pH 7.3 with NaOH). Neuromasts were ablated by submerging larvae in 10% Hanks' solution containing 400 mM neomycin (Fisher Scientific, Hampton, NH) for 1 h. We visually confirmed the ablation of neuromasts in a subset of larvae using an Olympus MVX10 (Tokyo, Japan) fluorescence microscope. To make neuromasts more visible under the microscope, larvae were exposed to 0.5 mM 2-(-4-dimethylaminostyryl)-*N*-ethylpyridinium iodide (Sigma Alrdrich, St. Louis, MO) in 10% Hanks' solution for 10 min. After neuromast ablation, larvae were moved to Hanks' solution to recover for at least 1 h.

Peripheral motoneuron recordings. Extracellular recordings from axial motoneurons were obtained with borosilicate glass pipettes (G150-F3, inner diameter: 0.86 mm, outer diameter: 1.55 mm, Warner Instruments, Hamden, CT) pulled with a P-97 Flaming/Brown micropipette puller (Sutter Instruments, Novato, CA). To construct pipette tips of an appropriate diameter to record from motoneurons (~30 μm), the fine pipette tips were manually broken off and then flame polished with a MF-830 microforge (Narishige, Tokyo, Japan). Pipettes were then filled with extracellular solution (134 mM NaCl, 2.9 mM KCl, 1.2 mM $MgCl_2$, 2.1 mM $CaCl_2$, 10 mM glucose, 10 mM HEPES buffer, adjusted to a pH of 7.8 with NaOH). Prior to recording, larvae were paralyzed by exposing them to 0.1% lyophilized α-bungarotoxin (Biotoxins, St. Cloud, FL) in 10% Hanks' solution for 5–10 min and then pinned on their side in a Sylgard-lined dish (Fluorodish, WPI, Sarasota, FL) containing extracellular solution. A section of skin spanning 3–5 myotomes was removed. The preparation was then placed under a ×40 objective microscope (Olympus BX51W1, Tokyo, Japan), and a recording pipette was placed on the exposed intermyotomal clefts using a four-axis automated manipulator (Siskiyou, Grants Pass, OR). The exposed muscle was gently drawn against the pipette by applying negative pressure of 10–30 mmHg (DPM1B pneumatic transducer, Fluke, Everett, WA). Signals were recorded with a sampling rate of 20 kHz using a MultiClamp 700B amplifier, a Digidata 1440A AD-converter (Axon CNS, Molecular Devices, Sunnyvale, CA) and MultiClamp 700B and Clampex 10.2 software.

Afferent neuron recordings. Loose patch recordings from lateral line afferent neurons were obtained in larvae prepared as described above. The same glass was used and pulled to ~3 MΩ resistance. Using DIC optics, the patch pipette was driven through the skin and into the posterior lateral line (PLL) ganglion using a 4-axis micromanipulator (Siskiyou, Grants Pass, OR). Light positive pressure of 30–50 mmHg was applied with a pneumatic transducer (model DPM1B, Fluke Biomedical, Everett, WA) during this process and while breaking into the ganglion. When the pipette was positioned against the soma of an afferent neuron, pressure was slowly decreased, and a negative pressure of 10–20 mmHg was applied to draw the cell against the pipette. Recordings were obtained in current clamp configuration with a 20-kHz sampling rate and 1k amplification using the same equipment as described for peripheral motoneuron recordings. The majority of motoneuron and lateral line afferent recordings was not obtained simultaneously, since the presence of two recording electrodes made it difficult to systematically stimulate all neuromasts. In three cases, simultaneous recordings from peripheral motoneurons and afferent neurons in the lateral line ganglion were obtained. In all cases, one of the recordings was lost before the stimulation protocol could be completed.

Neuromast stimulation. Controlled mechanical deflections of individual neuromasts were accomplished by using a blunt, flame-polished glass pipette with a tip diameter of ~20 μm. The pipette was attached to a head stage controlled by a piezo electric device (PX100, Piezosystemsjena, Jena, Germany) mounted onto a micromanipulator (WPI, Sarasota, FL). A preset ramp stimulus driving the displacement amplitude and velocity of the pipette was digitally controlled through Clampex 10.2 software and a Digidata 1440A AD converter. To stimulate a single neuromast, the tip of the glass pipette was brought near the cupula under the microscope. Spontaneous activity was recorded for 10 s before the stimulus; the cupula was then deflected by 0.3–30 μm at varied durations of 1–5,000 ms (deflection phase) and kept deflected for 5 s (stationary phase). The tip was then returned to its original position (release phase) with the same duration as used during the deflection phase, and activity was recorded for at least another 10 s. Rest period between stimulations was at least 1 min. To assess the effect of stimulation velocity on afferent response strength and fictive swimming probability, a constant deflection distance of 30 μm was used. This distance was determined to be sufficient to elicit a maximal response based on our results. All stimulation experiments were performed in a still-water bath without saline perfusion.

Electrical stimulation. As a control, we recorded peripheral motoneuron responses to electrical stimulation to evaluate the effect of a powerful sensory stimulus on motor behavior (Liao and Fetcho 2008). Electrical stimuli of 50–70 V were delivered through a bipolar electrode placed against the skin of the swim bladder region using a stimulus generator (Digitimer DS2A, Hertfordshire, UK).

Video confirmation of neuromast stimulation. The intended effect of our ramp command to the stimulation pipette, and therefore neuromast deflection, was confirmed by recording high-speed videos using a Phantom Miro EX-4 charge-coupled device camera at 200 frames/s (Vision Research, Wayne, NJ). Videos were analyzed using Phantom Camera Control Panel software and Image J (National Institutes of Health, Bethesda, MD).

Data analysis and statistics. Data analysis was performed using customized scripts written in Matlab version R2010a (The Mathworks, Natick, MA). For afferent recordings, a potential spike event was identified when voltage values fell between predetermined lower and upper thresholds. Spikes were considered if they exhibited a minimum duration of 0.01 ms and minimum interspike interval of 0.1 ms. Spike times were estimated from the onset of each spike. A spike density function was used to characterize the spike train, computed by convolving the spike train with a Gaussian kernel ($\sigma = 0.5$) over a 0.2-s window. To evaluate the strength of the evoked response, maximum spike rate was determined as the maximum value of the spike density function within a 1-s interval after stimulation offset. If the magnitude of the maximum spike rate was less than 3 standard deviations of the spontaneous spike rate, the data set was excluded from further analysis. The time delay between the stimulus onset and maximum spike rate, as well as 50% rise time (rise time from half-maximum to maximum spike rate) and 50% fall time (decay time from maximum spike rate to half-maximum), were measured to describe the kinetics of the response (Fig. 1). The delay between stimulus onset and 25% of the maximum afferent spike rate was used to characterize response onset (latency). At this point, evoked activity becomes distinguishable from spontaneous activity. Response probability for the afferent neurons was calculated as the ratio between responses and total number of trials in the given recording.

Motor responses (fictive swimming) were measured by recording extracellularly from peripheral motoneurons. For the motoneuron recordings, spikes were detected as described for afferent recordings. A swimming burst was defined as a segment of the spike train containing at least two spikes with a maximum interspike interval of 5 ms. A swimming bout was defined as a sequence containing at least two motor bursts with maximum interburst interval of 75 ms. We defined motoneuron activity as evoked when at least one swimming bout was detected within a 100-ms interval after stimulation offset. Response probability was computed by dividing the number of trials with responses by the total number of trials performed. Response latency was defined as the time delay between stimulation onset and the first burst activity in the first swimming bout. Instantaneous burst frequencies were derived from interburst intervals by measuring the time interval between the midpoints of each burst. Mean burst frequency of a swimming bout was estimated by dividing the total number of bursts by the duration of the swimming bout. Swimming bout duration was determined using the onset of the first swimming burst and the offset of the last burst. Duty cycle for a swimming bout

was estimated as the ratio between the total burst duration and the swimming bout duration. Instantaneous and mean burst frequency, duration of the first swimming bout and duty cycle of motoneuron recordings were analyzed across deflection velocities and compared with those of spontaneous and electrically stimulated motoneuron activity. To determine whether there were differences between evoked (lateral line or electric) motor activity or spontaneous activity, statistical tests were performed in Matlab with a significance level of $P \leq 0.05$. Pairwise comparisons were tested using paired or unpaired *T*-tests and Bonferroni corrected for multiple comparisons, as appropriate. Probabilities were compared using Fisher's exact test.

The relationship between motor response probability or maximum spike rate and deflection velocity was linear at intermediate deflection velocities and plateaued at lower and higher velocities. To describe this relationship we fitted the data with the equation:

$$y = \frac{ABx}{1 + Bx} + C \quad (1)$$

where coefficients *A*, *B* and *C* were estimated using least square methods. Five temporal measurements (response latency of both motoneurons and afferent recordings, time delay between maximum spike rate and stimulation onset, 25% rise time, 50% rise time and 50% fall time of afferent recordings) were modeled as a reciprocal function of deflection velocity:

$$y = \frac{A}{x} + B \quad (2)$$

where coefficient *A* corresponded to the relative deflection distance of the cupula for a given temporal measurement. Thus, if we apply *Eq. 2* to the response latency measurement, then coefficient *A* corresponds to the deflection amplitude at which the spike rate of an afferent reaches above its spontaneous level. When we apply *Eq. 2* to the time to maximum response measurement, then coefficient *A* corresponds to the deflection amplitude to which an afferent reaches its maximum spike rate. Performance of the models was evaluated using the values of coefficients of determination (R^2). We furthermore related the motoneuron activity to afferent activity by identifying the relationship between afferent maximum spike rate and motoneuron response probability, as well as time delay of afferent maximum spike rate and motoneuron response latency with respect to stimulation onset using linear regression.

Neuromasts in the PLL were divided into four sections to look for regional differences in elicited swimming response probabilities: the dorsal lateral line containing D1–D3, the rostral lateral line containing L1, L2 and LII.1–LII.3, the median lateral line containing L3 and L4, and the caudal lateral line containing L5 and the terminal neuromasts (Fig. 1*A*). In addition, we stimulated neuromasts in the anterior lateral line system to compare it to the results we found for the PLL.

RESULTS

At 5 dpf, zebrafish larvae can already use their superficial neuromasts to sense water flow and initiate swimming in response to flow stimuli (McHenry et al. 2009; Olszewski et al. 2012). While superficial neuromasts have long been known to respond to flow stimuli (Dijkgraaf 1963; Sand 1937; Schulze 1870), we still do not know exactly how deflection of superficial neuromasts translates into an afferent response and ulti-

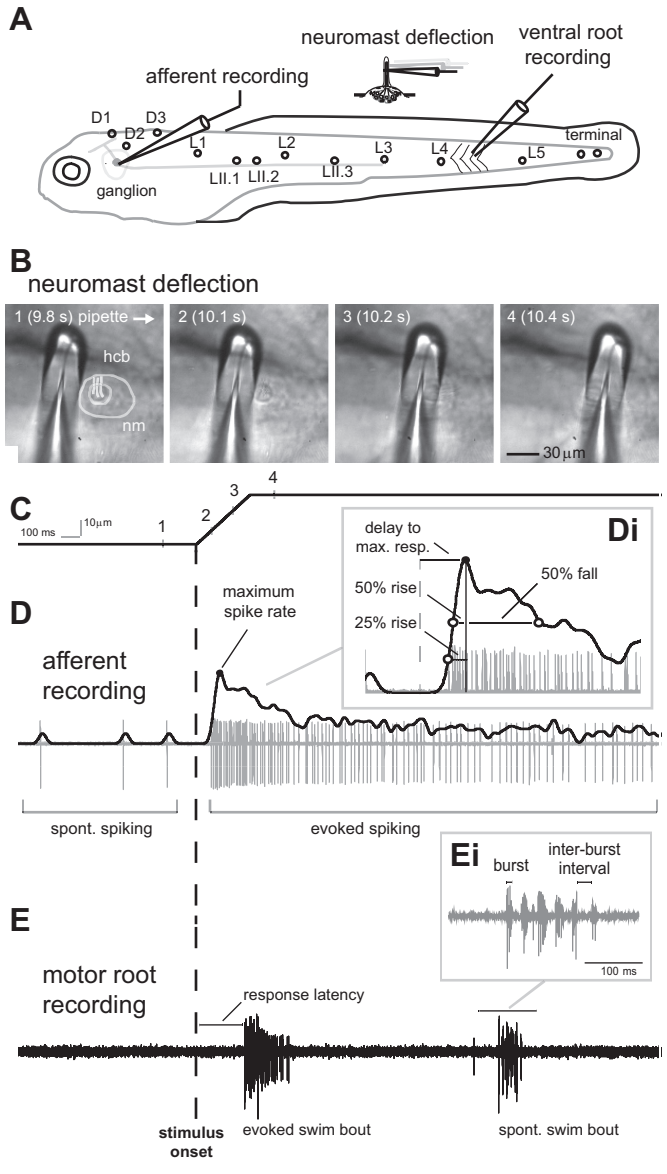

Fig. 1. In vivo recordings of posterior lateral line (PLL) afferent neuron activity and axial motor activity in larval zebrafish in response to mechanical deflection of the cupula in a single neuromast. *A*: 5-day postfertilization larvae have identifiable neuromasts (D1–3, L1–3. LII.1–3) innervated by afferent neurons with somata located in the PLL ganglion. Afferent activity was recorded at the somata with loose patch recordings, while the connected neuromast was identified and then the cupula was carefully deflected with a glass pipette. In separate experiments, we evaluated the effect of cupula deflection on motor output by performing extracellular recordings from peripheral motoneurons with suction electrodes. *B*: image sequence showing the cupula of a neuromast (L3) being deflected along the caudo-rostral axis of the body. Image *frames 1–4* correspond to time points along the ramp stimulus shown below. The neuromast (nm) and hair cell bundle (hcb) are outlined for clarity in *image 1*. *C*: to stimulate a neuromast, we presented a ramp command to control the movement of a glass pipette. Data are presented in the same time scale; the onset of the pipette movement is represented by the vertical dashed line in *C–E*. This setup allowed us to systematically change the deflection velocity. *D*: example of an afferent spike train and estimated spike rate (solid black line), showing the spontaneous (SP) and evoked spike rate relative to the stimulus onset. *Di*: the delay between stimulus onset (dashed line) and maximum spike rate (black circle), time between half-maximum spike rates and maximum spike rate before and after the peak (50% rise and fall, respectively), as well as 25% rise time (open circle) were determined to characterize the temporal structure of the response. *E*: extracellular recordings from peripheral motoneurons revealed that the deflection of the cupula in a single neuromast could elicit fictive swimming. Swimming response latency, swimming bout duration, mean burst frequency, and burst duration were calculated to compare lateral line (LL) evoked, electrically evoked (EL) swimming and SP swimming. *Ei*: burst duration and interburst interval of a SP swimming bout.

mately to motor behavior. To better understand the mechanisms of sensorimotor integration, we developed an in vivo preparation to record activity from individual afferent neurons as well as peripheral motoneuron activity while selectively stimulating a single, connected neuromast in the PLL system (Fig. 1*A*). When the cupula in an appropriate neuromast was deflected using a ramp stimulus (Fig. 1, *B* and *C*), we observed adapting responses in afferent neurons. Specifically, spike rate increased quickly to reach a maximum, after which it exhibited a gradual decrease but still remained above spontaneous spike rate levels (Fig. 1*D*). We determined the 50% rise and fall times to characterize the response slope and describe the temporal dynamics of the afferent responses (Fig. 1*Di*).

When we recorded from the peripheral motoneurons, we found that swimming bouts were evoked by the deflection of the cupula in a single neuromast (Fig. 1*E*). Besides evoked swimming bouts, also spontaneous swimming bouts that occurred in absence of any neuromast stimulation (Fig. 1*Ei*) were observed.

Each PLL afferent neuron is functionally connected to three neuromasts or less. We recorded from 20 units in 16 larvae to categorize the responses of PLL afferent neurons to mechanical stimulations of individual neuromasts. After a recording from an afferent cell body was established, the connected neuromasts were located by systematically deflecting the cupula of each visible neuromast on the body along the rostro-caudal axis with a test velocity of 0.06 μm/ms. We confirmed that neuromasts could be selectively stimulated, since we typically observed an afferent unit response to stimulation of one or sequential stimulation of a few neighboring neuromasts at a time (Fig. 2, *A* and *B*). In 11 out of 20 recorded units, we obtained responses from one neuromast, in four cases from two neuromasts that were stimulated one after the other, and in one case from three neighboring neuromasts that were stimulated sequentially. In four units, spontaneous activity, but no response to neuromast stimulation was observed. The fact that a single afferent can be connected to multiple neuromasts is in agreement with previous anatomical studies (Haehnel et al. 2011; Nagiel et al. 2008). Overall, 12 recorded units exhibited excitatory responses to the deflection phase and 4 units to the release phase (rebound after inhibition), while 4 units did not respond to any of our stimulations. Since the majority of units responded to the deflection phase, we concentrated our analysis on these units. It is possible that more afferent neurons innervate head to tail sensitive hair cells, since this should be the primary axis of hydrodynamic stimulation by flow for fish swimming forward. Once an excitatory response was observed, a range of deflection velocities was applied. In general, spike rate increased with deflection velocity, while latency decreased (Fig. 2*C*).

Response properties of afferent neurons to stimulation of individual neuromasts. For each recording, we measured how afferent spike rate increased with cupula deflection velocity at a constant deflection distance of 30 μm and fitted the data with *Eq. 1* (Fig. 3*A*). Spike rate increased linearly within a range of deflection velocities between 0.1 and 1.0 μm/ms and then plateaued at higher velocities. At the lowest deflection velocity of 0.006 μm/ms, spike rates were ~25% higher than the spontaneous spike rate. To describe different response dynamics, the characteristic response parameters, such as latency, response maximum and 50% rise and fall time, were assessed as a function of deflection velocity (Fig. 3, *B*, *C*, *E*, and *F*). To fit the data, a reciprocal function of the deflection velocity was used (*Eq. 2*, see MATERIAL AND METHODS). Coefficient *A* in this function represents an estimated constant deflection distance at which the measured parameter was observed across deflection velocities. We found that response latency decreased with increasing deflection velocity (Fig. 3*B*). We fitted this data with *Eq. 2* to determine the minimum deflection distance that elicits

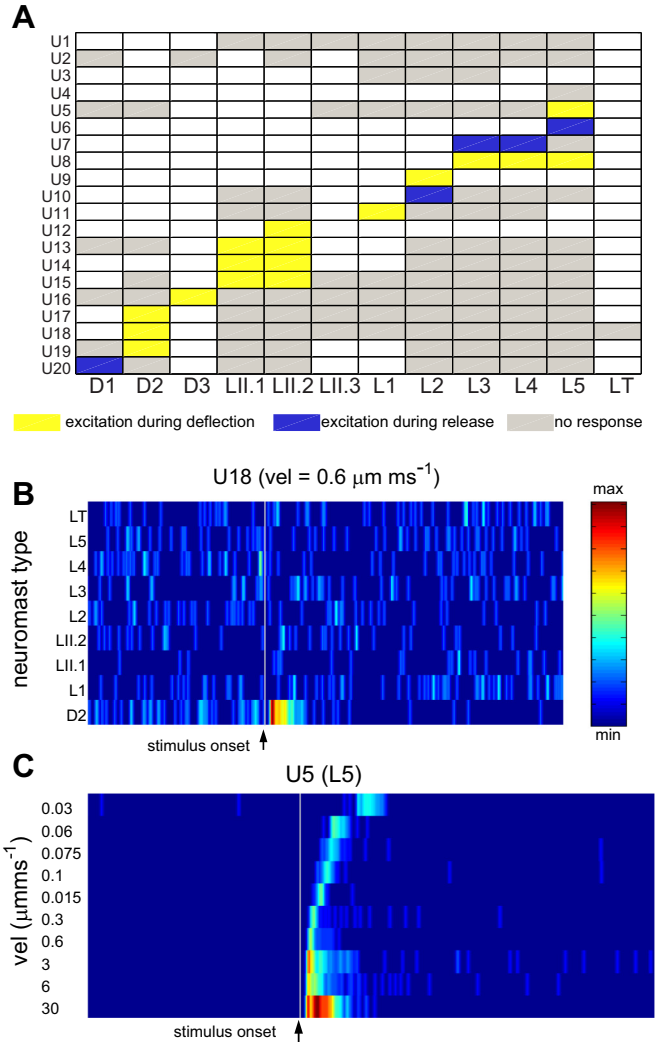

Fig. 2. Responses of PLL afferent neurons to stimulation of specific neuromasts. *A*: data matrix showing responses of 20 LL afferent units (U1–20) to deflections of the cupula in individual neuromasts along the rostro-caudal axis of the body. Each unit typically responds only to stimulation of one or two adjacent neuromasts, where stimulation of other neuromasts elicited no response (gray boxes). Most responses consisted of an excitatory (increased spike rate) response during the deflection phase (yellow boxes). In some cases, an excitatory response (rebound from inhibition) was detected only during the release from deflection (blue boxes). For this study, we focused our analysis on responses observed during the deflection phase. White boxes correspond to neuromasts which were not tested. *B*: example of raster plot of normalized spike rates (from U18 in *A*) showing that this afferent unit responds selectively to stimulation of the D2 neuromast. The vertical gray line represents the stimulus onset. Each row represents the spike rate observed in response to the deflections of the cupula in a specific neuromast with a ramp stimulus of 0.6 μm/ms velocity. *C*: example of an afferent unit showing responses to ramp stimulations across different deflection velocities (corresponding to U5 responding to stimulation of neuromast L5). Note that spike rate increases as deflection velocity increases, while response latency decreases.

afferent activity (i.e., afferent spike rate exceeds spontaneous spike rate by 25%), which was 7.7 μm. This suggests that, to observe afferent activity, the cupula should be deflected by at least ~8 μm, on the basis of the used threshold criterion.

We then asked what was the minimum cupular deflection required by the afferent neuron to reach its maximum spike rate. Again, by using *Eq. 2*, we estimated that the maximum spike rate occurred at a deflection distance of 14.3 μm (Fig. 3*C*). This distance corresponds to about one-half of the deflection distance (30 μm) that was applied for this set of experiments. From these experiments, we conclude that afferent neurons are most sensitive to cupula deflections between ~8 and 14 μm. In other words, when the cupula is deflected by <8 μm, there is very little increase in afferent spike rate compared with the spontaneous spike rate, regardless of deflection velocity. When the cupula is deflected by >14 μm, there is very little difference in spike rate with respect to the maximum spike rate.

We were surprised that an afferent neuron could not detect deflections of <8 μm, given the submicron sensitivity of hair cells reported in other systems (van Netten 2006). We were concerned that these results may be specific to the stimulation protocol we used, so we designed a second experiment to independently evaluate this 8-μm threshold. We directly deflected the cupula in single neuromasts by <8 μm to see if there was any increase in spike rate compared with spontaneous activity. Positive responses (i.e., evoked spike rate >25% above the spontaneous spike rate) were tallied over many trials to determine the overall response probability, which is calculated as a percentage of positive responses to the number of trials. We tested four such deflection amplitudes: 0.3, 1.5, 3.0 and 30 μm (Fig. 3*D*). For each pair of comparisons, deflection velocity was held constant. We found that, for all three deflection amplitudes, the response probability was <25%. In contrast, the 30-μm control deflection elicited a response probability of >70%. Our initial estimation of an 8-μm threshold

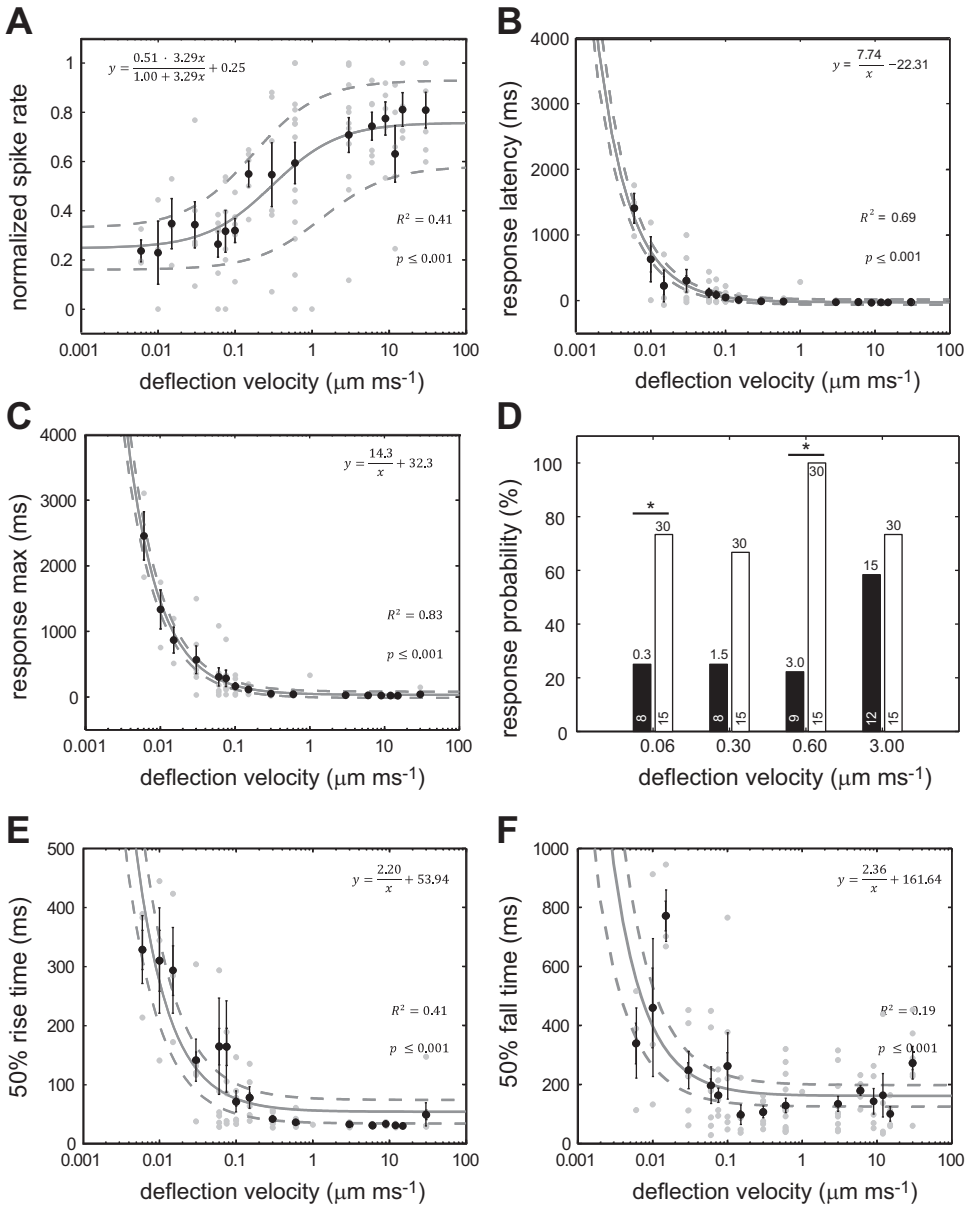

Fig. 3. The response of afferent neurons to cupula deflection velocity. *A*: normalized mean spike rate increases with deflection velocity, showing a linear relationship within an intermediate velocity range (0.1–1.0 μm/ms). *B*: response latency decreases with increasing deflection velocity. *Equation 2* is applied to the data to predict the minimum deflection distance (7.74 μm) that is needed to elicit a response. *C*: time to maximum response decreases as velocity increases and saturates above 0.1 μm/ms to a value of 32.3 ms. *Equation 2* is applied to the data to predict how an afferent neuron encodes deflection velocity. Afferent activity reaches its maximum at a deflection distance of 14.3 μm, after which spike rate saturates. *D*: comparison of afferent response probability to small and large deflections distances (black and white bars, respectively). Deflection distance (μm) is indicated at the *top* of each bar, and the sample size is indicated at the *bottom* of each bar. *Significance at $P \le 0.05$, Fisher's exact test (for deflection velocity 0.3 μm/ms, $P = 0.009$). *E*: 50% rise time decreases with increasing deflection velocity and saturates above 0.1 μm/ms to a value of 53.94 ms. *F*: 50% decay time also decreases with increasing deflection velocity and saturates above 0.1 μm/ms to a value of 161.64 ms, but shows more variance at faster deflection velocities. In all panels except *D*, black circles represent mean values ± SE, gray circles indicate individual values and the solid line indicates fitted model with 95% confidence interval (dashed lines); n = 8–10 recorded units per velocity. The equations describing the data for all figures except *D* are presented in each corresponding panel.

was confirmed, given that the response probability was low and was constant for these deflection amplitudes. As an additional control, we used a deflection distance that was >8 μm. We chose a 15-μm deflection and found that it elicited a similar response probability as a 30-μm deflection.

To better analyze afferent response kinetics, we also computed the 50% rise and fall time across deflection velocities, both of which decreased as deflection velocity increased (Fig. 3, *E* and *F*). At low deflection velocities (<0.01 μm/ms), the estimated rise time was one-half that of the fall time. At high deflection velocities (>0.01 μm/ms), the estimated rise time was one third that of the fall time. This indicates asymmetric response kinetics in which the rising slope was steeper than the trailing slope. Overall, our results demonstrate that afferent activity can be described as an adaptive response which becomes faster and stronger with deflection velocity.

Fictive swimming responses to mechanical deflection of individual neuromasts. We found that deflection of a single neuromast could generate a reliable fictive swimming response. The probability of eliciting swimming increased from 20% to ~80% when neuromast deflection velocity increased (Fig. 4*A*). We presented the same stimulation protocol to a control group of larvae with chemically ablated neuromasts, positioning the pipette along the skin where neuromasts would be located in intact larvae. When we did this, we observed substantially reduced swimming responses. Interestingly, at high velocities, we still observed swimming responses in lateral line ablated larvae. We speculate that at high velocities the movement of the pipette through water generates multimodal cues that may stimulate the somatosensory or auditory system. In a control configuration, we used a strong electrical stimulus and found no difference in swimming response probabilities between intact and ablated larvae. The response probability to electrical stimulation exceeded that of lateral line stimulation.

We found that response probabilities evoked by stimulation of PLL neuromasts were significantly higher than those evoked by stimulation of anterior lateral line neuromasts (Fig. 4*B*). We next tested if certain regions within the PLL were more likely to evoke a swimming response than others, since caudal neuromasts have been shown to play a larger role in evoking swimming avoidance responses in freely moving larvae (Olszewski et al. 2012). We subdivided the PLL into four regions but found no significant differences in response probabilities among these regions (Fig. 4*B*).

To characterize lateral line evoked swimming, we next compared a variety of swimming parameters to look for differences between spontaneous swimming, swimming evoked

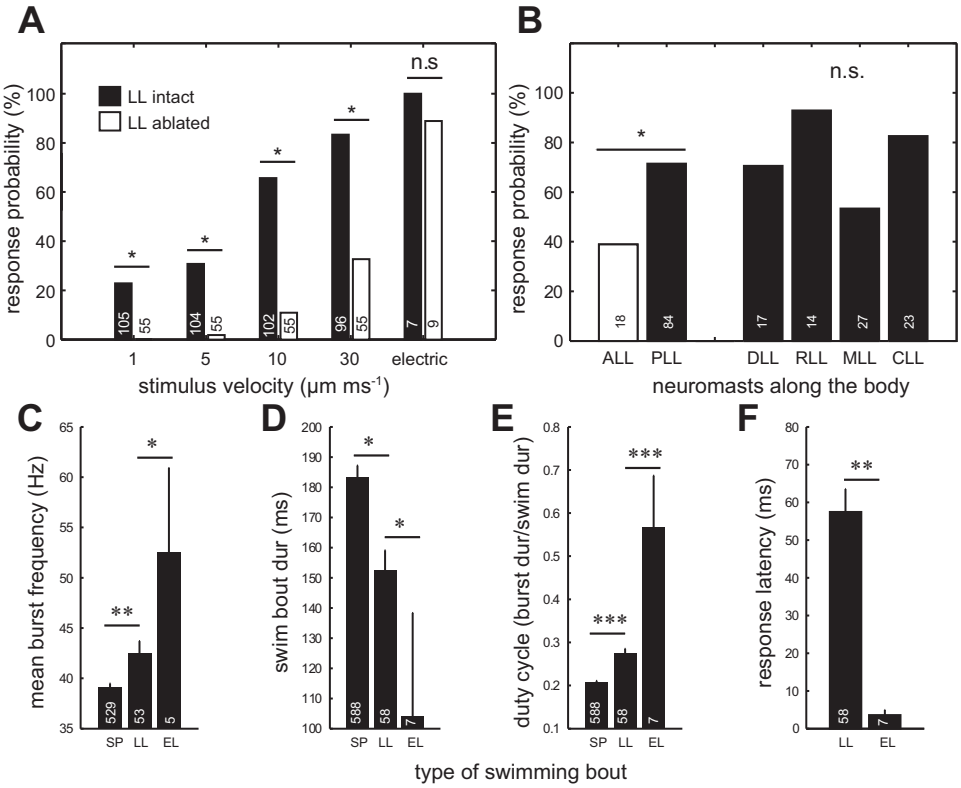

Fig. 4. The probability of eliciting swimming in response to cupula deflections in individual neuromasts. *A*: swimming response probabilities increase with cupula deflection velocity and become most reliable at very high velocities. Larvae with an ablated LL show lower swimming probabilities. As a control, an electrical stimulus was used and indicated no difference in swimming responses between intact and LL ablated larvae. *B*: response probabilities for high velocity of 10 μm/ms cupula deflections from different body regions. There is a higher response probability for stimulation of neuromasts in the PLL than for neuromasts in the anterior LL (ALL). There were no differences in responses when we stimulated neuromasts from four subregions within the PLL: the dorsal LL (DLL), the rostral LL (RLL), the median LL (MLL) and the caudal LL (CLL). Comparison of PLL regions were Bonferroni corrected, all P values > 0.008. *C*: mean burst frequencies for LL evoked swimming bouts were higher than for SP swimming bouts, but lower than for EL swimming bouts. *D*: mean swimming bout duration was longest for SP swimming, followed by LL evoked and EL swimming. *E*: mean duty cycle for LL evoked swimming was higher than for SP swimming but lower than for EL swimming. *F*: the motor response to LL stimulation occurred much later than the response to electric stimulation. *C–F*: unpaired *T*-test: *$P \leq 0.05$, **$P \leq 0.01$, ***$P \leq 0.001$. For all plots, sample sizes are indicated at the *bottom* of each bar.

by individual neuromast deflection, and swimming evoked by electric stimulation. Previous studies have compared spontaneous swimming bouts with light-evoked swimming (Masino and Fetcho 2005) and characterized electrically stimulated escape responses (Liu et al. 2012). Here, we wanted to characterize lateral line evoked swimming relative to spontaneous swimming and escape responses. We discovered that mean burst frequency was highest for swimming bouts evoked electrically (52.5 ± 8.4 Hz), followed by lateral line evoked swimming (42.5 ± 1.2 Hz) and spontaneous swimming (37.1 ± 0.4 Hz) (Fig. 4*C*). Swim bout duration was longest for spontaneous swimming (183.1 ± 4.0 ms), followed by lateral line evoked swimming (152.3 ± 6.8 ms) and then electrically evoked swimming (104.2 ± 34.1 ms) (Fig. 4*D*). Duty cycle was greatest for electrically evoked swimming (0.6 ± 0.1), followed by lateral line evoked swimming (0.3 ± 0.0) and then spontaneous swimming (0.2 ± 0.0) (Fig. 4*E*). Response latency for electrically evoked swimming (3.6 ± 1.4 ms) was ~15 times shorter than for lateral line evoked swimming (57.5 ± 6.1 ms) (Fig. 4*F*). Overall, lateral line evoked swimming had intermediate values between spontaneous and electrically stimulated swimming.

We then looked at the effect of neuromast deflection velocity on the probability to elicit a swimming response. By fitting the response probabilities to increasing deflection velocities (at a constant deflection distance of 30 μm) using *Eq. 1*, we found that the probability of swimming was ~30% for the lowest deflection velocities and plateaued at ~80% for the highest deflection velocities (Fig. 5*A*). Response latency decreased with increasing deflection velocity and reached its shortest value of 47 ms at the highest deflection velocities (Fig. 5*B*). We found that high velocities elicited higher instantaneous burst frequencies for the first two swimming bursts compared with spontaneous swimming. In contrast, we found no such differences when neuromasts were deflected at low velocities. Figure 5, *C* and *D*, shows representative examples of instantaneous burst frequencies plotted against burst number for one high and one low deflection velocity. Since most of the differences between evoked and spontaneous swimming occurred within the first three bursts, we compared the frequencies of these bursts for all deflection velocities (Fig. 5*E*). We found that, for lower velocities (<0.3 μm/ms), there was no difference between evoked and spontaneous swimming. In contrast, at higher velocities (≥0.3 μm/ms), the first two burst frequencies

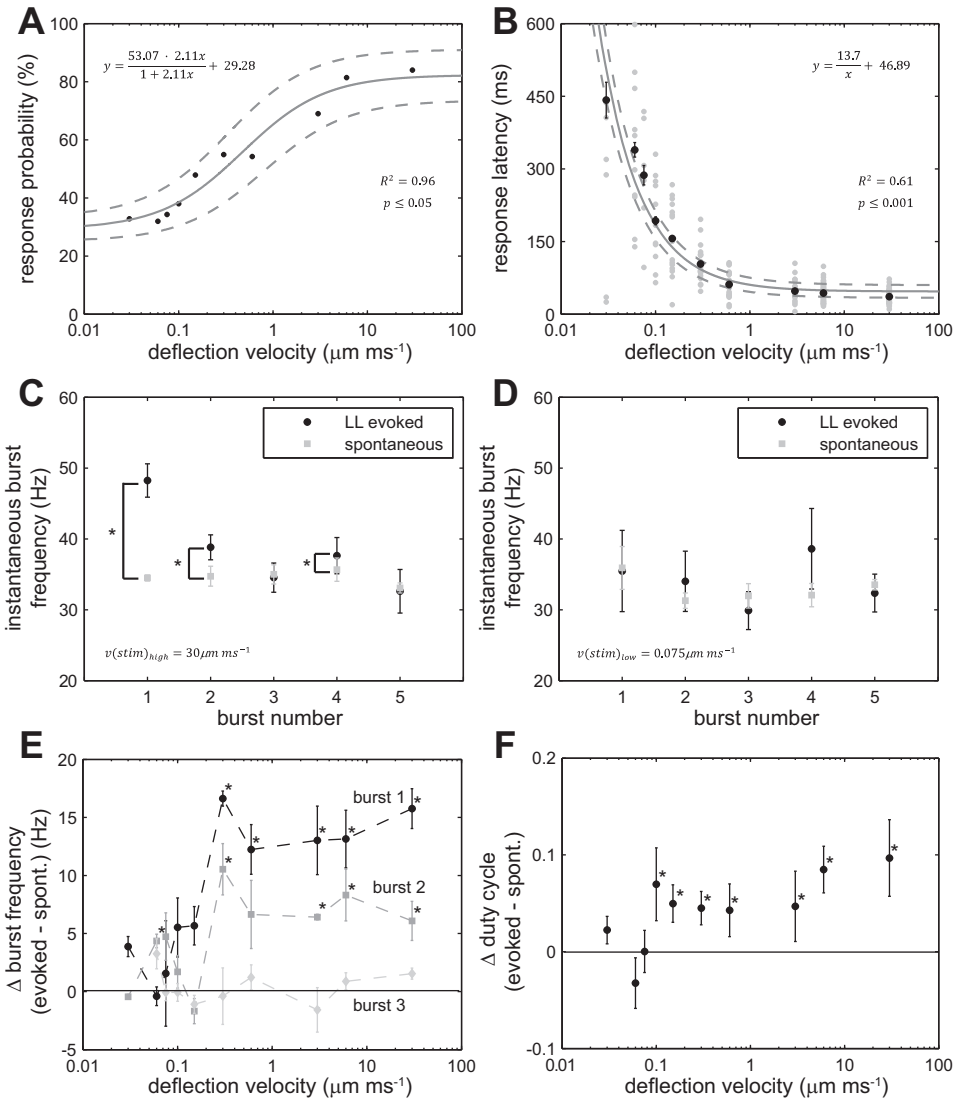

Fig. 5. Swimming parameters in response to mechanical deflection of the cupula in individual PLL neuromasts. *A*: swimming response probability increased with deflection velocity (black circles represent probabilities pooled for all neuromasts). Solid line represents fitted model with 95% confidence interval (dashed lines), $67 \le n \le 72$ trials per velocity, where each larva was tested once. *B*: swimming response latency decreased with deflection velocity (black circles represent mean latencies for positive responses ± SE, gray circles represent individual latencies). Solid line represents fitted model with 95% confidence intervals (dashed lines), $9 \le n \le 49$ swimming responses per velocity. *C*: a comparison of instantaneous burst frequency for the first five bursts during the initial swim bout of LL evoked swimming and SP swimming. A high velocity deflection (30 μm/ms) evoked a higher swimming frequency for the first two bursts compared with SP swimming (mean burst frequency ± SE; $^*P \le 0.05$, paired *T*-test, $n = 49$). *D*: the same comparison using a low velocity deflection (0.075 μm/ms) showed no difference in frequency for all five swimming bursts ($n = 17$). *E*: differences in LL evoked and SP swimming were evident for the first and second burst, for deflection velocities ≥0.3 μm/ms (mean instantaneous evoked burst frequency − mean instantaneous SP burst frequency ± SE, $9 \le n \le 49$ per velocity, $^*P \le 0.05$, *T*-test comparing evoked and SP instantaneous burst frequencies). *F*: the differences in duty cycle between SP and evoked swimming are plotted across deflection velocities. Duty cycle for LL evoked swimming at higher stimulation velocities (>0.1 μm/ms) was higher than for SP swimming (evoked mean duty cycle − SP mean duty cycle ± SE, $9 \le n \le 49$ per velocity, $^*P \le 0.05$, *T*-test comparing evoked and SP duty cycles). In *E* and *F* line: $y = 0$, represents no difference.

of evoked swimming were higher than for spontaneous swimming. In Fig. 5*F*, the differences between duty cycle of spontaneous and evoked swimming bouts are plotted across deflection velocities. Again, for lower velocities (<0.15 μm/ms), there was no significant difference in duty cycle between evoked and spontaneous swimming. At higher velocities (≥0.15 μm/ms), the duty cycle for evoked swimming was higher than for spontaneous swimming (Fig. 5*F*). Thus swimming responses to fast neuromast deflections are characterized by a higher initial burst frequency and duty cycle and can be readily distinguished from spontaneous swimming. A transition from spontaneous to evoked swimming occurs at an intermediate velocity range between 0.15 and 0.3 μm/ms.

Relationship between sensory and motor responses to neuromast stimulation. We have discovered that mechanical stimulation of individual neuromasts in the lateral line system, regardless of its location along the body, reliably evokes swimming motor responses in larval zebrafish. In addition, we have demonstrated that neuromast deflection predictably evokes responses in lateral line afferent neurons prior to the motor response (Fig. 1). We are, therefore, in a unique position to understand the sensory representation of a lateral line stimulus at the single cell level, as well as survey the potential of a stimulus of a particular magnitude to evoke swimming. We took advantage of this opportunity by characterizing how lateral line afferent activity is related to swimming activity. When we plotted response probability for motoneuron activity against the normalized maximum spike rate of afferent neurons, we found that swimming probability increased linearly with increasing spike rate (Fig. 6*A*). These data demonstrate that, once an afferent neuron reaches ~15% of its maximum spike rate, the probability to elicit a swimming response rises above the spontaneous level. As expected, afferent neurons responded to a neuromast deflection first, and followed by the swimming response ~25 ms later (Fig. 6*B*). Motor responses were recorded 8–12 segments away from the afferent ganglion. A previous study (Masino and Fetcho 2005) reported a segmental delay of 0.8 ± 0.5 ms per segment for the rostro-caudal progression of spontaneous swimming (35.6 ± 4.7 Hz). Assuming that lateral line evoked swimming progresses rotrocaudally, an additional delay of up to ±4 ms ± 63% has to be considered. We confirmed that the afferent response preceded the peripheral motoneuron response in simultaneous recordings from afferent neurons at the ganglion and motoneurons at a segment rostral to the stimulated segment (Fig. 6*C*).

DISCUSSION

Deflection of the cupula in a single neuromast can elicit a swimming response. Our findings reveal an unexpected sensitivity in the larval PLL system; an appropriate mechanical deflection of the cupula in a single neuromast can elicit a swimming response. Given that there are far fewer neuromasts in larvae compared with adults, it is perhaps not surprising that we see such high gain in the larval lateral line system. A similarly remarkable sensitivity has been recently described for the somatosensory system in larval zebrafish, where a single spike elicits a swimming response (Douglass et al. 2008). We can envision two advantages to this capability. First, it allows larvae the capacity to exhibit diverse behaviors (e.g., foraging, avoidance, etc.) by simply reacting to complex stimuli in their hydrodynamic environment. Specifically, if we treat the swimming response elicited by single neuromast stimulation as a behavioral building block, this swimming response can be transformed into complex behaviors based on spatially and temporally distributed hydrodynamic cues. Second, it provides a foundation to be able to generate more powerful behaviors, such as an escape response through the stimulation of multiple neuromasts. It has been shown that stronger stimuli elicit escapes at the behavioral level in freely swimming larvae (Liu and Fetcho 1999).

We show that the motor response probability is correlated to afferent spike activity, where probability increases linearly

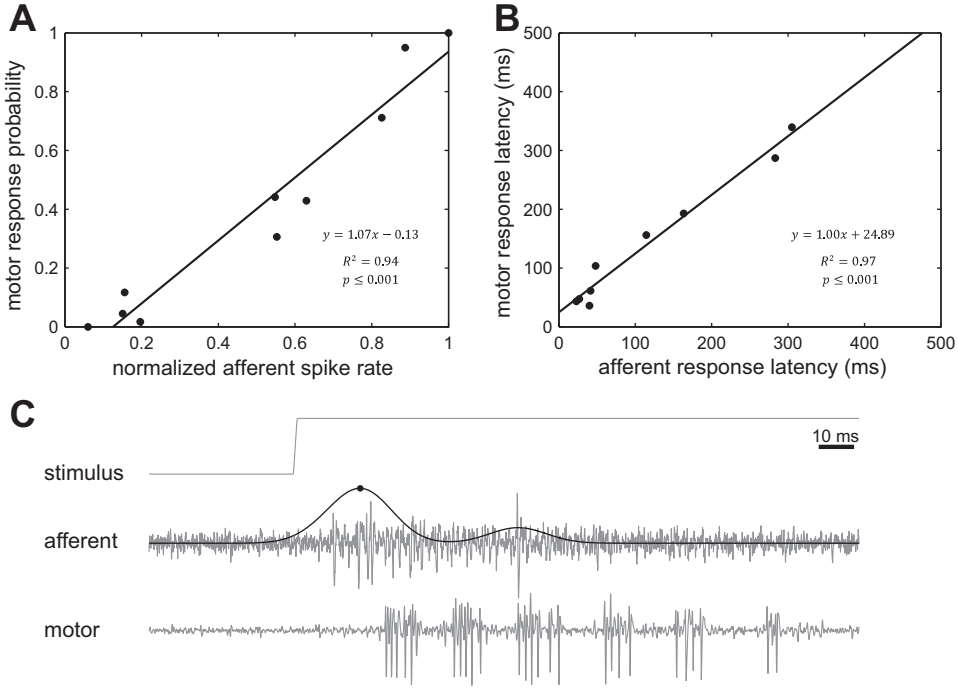

Fig. 6. A linear relationship exists between afferent neuron activity and swimming in response to deflections of the cupula in single neuromasts. *A*: probability of swimming response increased linearly with afferent spike rate and began to appear at 15% of the normalized maximum spike rate (black circles represent mean values). *B*: motor response latencies were slower as afferent responses to deflections became slower (black circles represent mean values). *C*: simultaneous recording of an afferent neuron and peripheral motoneurons while deflecting the cupula of connected neuromast. An example is shown to illustrate the delay between the maximum afferent response and motoneuron activity (solid line represents convoluted spike rate, black circle indicates maximum spike rate).

with spike rate. We propose a simple thresholding algorithm that can predict the afferent-motor activity relationship. This spike-timing algorithm counts the total number of spikes coming from the entire population of afferent neurons within a certain time interval. Once a certain number of spikes are reached, a command for motor activity proceeds. The underlying mechanism for this spike-timing algorithm could be that upstream neurons mediate gain control, based on coincidence detection. These hypothetical neurons would only discharge when they receive coincident spikes from lateral line afferent neurons. A mechanism like this is realized in the auditory system where cells in a binaural nucleus detect coincidental spikes from their monoaural excitatory afferents (Jeffress 1948). In this way, the decision to generate a motor response cannot be explained deterministically just by the activity of the stimulated afferent. We know this because, even when one afferent is maximally stimulated, there is still a 20% chance of not generating a motor response (Fig. 5*A*). Therefore, the activity of the stimulated afferent should be synchronized with the spontaneous activity of a subset of other afferents to push the system above threshold. If there is no coincidental spontaneous activity, then there is no motor response. The randomness of the spontaneous activity (Trapani and Nicolson 2011) imposes uncertainty onto the motor initiation process, which in turn is reflected in the probability response. When the deflection velocity increases, the spike rate of the corresponding afferent neuron also increases. This decreases the overall uncertainty of generating a motor response, as fewer spikes from other neurons are needed. This results in a higher probability of generating a motor response. Our coincidence algorithm could then be modeled with a computational model, such as the perceptron model, which is used in the machine learning field (Haykin 1998; Rosenblatt 1958).

If sensorimotor integration is additive, as described by our algorithm, then two or more neurons simultaneously firing at a low spike rate can achieve the same motor response probability as one neuron firing at a high spike rate. We propose that swimming can be initiated by the slow deflection of the cupula in multiple neuromasts innervated by more than one afferent as easily as the fast deflection of the cupula in a single neuromast. In this respect, the collective sensitivity of the lateral line system would be higher than the sensitivity of any one neuromast when it comes to generating a swimming response.

Lateral line evoked swimming is distinctive. Swimming responses to high-velocity cupula deflections were different from spontaneous swimming, as well as from responses to electrical stimulation, which elicits escapes (Liu et al. 2012). Given that the response latency of lateral line evoked swimming is around 60 ms, this suggests that the stimulation of a single neuromast does not elicit a Mauthner-initiated escape response, which has been shown to occur within 8 ms (Liu et al. 2012). This may be because the Mauthner cell requires multimodal sensory inputs to generate a C-start at this developmental stage (Kohashi et al. 2012). We also found that swimming in response to high-velocity deflections is more powerful (higher frequency and longer duty cycle) than light-evoked swimming (Masino and Fetcho 2005), which is similar to spontaneous swimming. However, there is no difference between spontaneous swimming and lateral line evoked swimming in response to low-velocity deflections. This is because at low-deflection velocities, we are simply observing spontaneous swimming and not actually evoking a motor response. Even though a low-velocity deflection is perceived by an afferent neuron, this signal is not translated into a motor response. We believe this to be the case because, even when we record motoneuron activity in the absence of any stimulation, we see spontaneous activity ~30% of the time. This value matches the response probability that we observe during low-velocity deflection, thereby suggesting that this motor activity arises by chance. Alternatively, we do evoke a motor response, but one which resembles spontaneous activity.

Adaptive response of afferent neurons to ramp stimulation of a neuromast. We believe that a situation in which steady flow interacts with a neuromast most closely mimics our ramp stimulation. A previous study had shown that, in one species of fish exposed to steady flow, lateral line afferent activity increased with flow velocity and exhibited nonadaptive, tonic responses (Voigt et al. 2000). This suggests that, even after flow reached a steady state, afferent neurons maintained their level of activity. In our study, we also see a linear relationship between afferent activity and cupula deflection velocity. However, when we physically held the cupula deflected, we observed a steady decline in afferent activity. This means that, in our study, afferent neurons were becoming less sensitive over time in response to a constant deflection amplitude. One explanation for this difference is that steady flows may not result in constant amplitudes in cupula deflection. In fact, steady flows have been shown to inherently contain micro fluctuations which can be detected by the lateral line (Chagnaud et al. 2008). These fluctuations can explain the nonadaptive tonic responses observed previously (Voigt et al. 2000). It may also be that the larval superficial neuromasts are putative canal neuromasts and have different response properties from adult superficial neuromasts.

We demonstrated that the spike rate of an afferent neuron increases linearly with deflection velocities between 0.1 and 1.0 μm/ms. For a 4-mm-long larva, this corresponds to a 0.025–0.25 body lengths per second (*L*/s). This suggests that, when a larva swims (~8–55 *L*/s) (Müller and van Leeuwen 2004), afferent activity should be heavily influenced by the self-motion of the animal. The adaptive response of afferent neurons observed in this study can be a mechanism to compensate for potential signal saturation.

Minimum cupula deflection amplitude required to evoke afferent activity. We discovered that a mechanical ramp stimulation of an individual neuromast >8 μm can elicit responses in a connected afferent neuron, which increase linearly with the velocity of cupula deflection. This is interesting because previous work in adult fish derived that the hair cells in a neuromast can be substantially more sensitive, with submicron detection thresholds (Kroese and Schellart 1992; van Netten 2006). However, the threshold to elicit an action potential in afferent neurons based on the deflection of the cupula can be different from the sensitivity of a single hair cell.

Also, larval zebrafish are small and swim in a very different hydrodynamic regime than adults, where viscosity dominates over inertial forces (McHenry and Liao 2014). A tighter coupling of the fluid to the cupula at low Reynolds numbers results in greater deflection amplitudes; to avoid overstimulation it may be beneficial for larvae to be less sensitive.

Direct mechanical stimulation of superficial neuromasts. Many lateral line studies have focused on the correlation of flow and afferent activity, using various stimuli that range from

moving spheres (Coombs and Janssen 1989; Denton and Gray 1983; Mogdans and Bleckman 1998; Trapani and Nicolson 2011), to bulk water flow (Engelmann et al. 2000; Voigt et al. 2000) and water jets (Dijkgraaf 1963; Goerner 1963; Liao 2010; Ricci et al. 2013). However, with these hydrodynamic stimuli come the challenges of validating their effect on the motion of the neuromast itself. Complex fluid-structure interactions prevent the dissection of the relationship between the fluid motion and the cupula and, subsequently, the motion of the cupula and afferent activity itself. Although some studies have characterized the fluid structure interactions for canal neuromasts more carefully using laser interferometry (van Netten 1987), the situation for superficial neuromasts is not as well understood (McHenry and Liao 2014).

To bypass complex fluid-structure interactions, the direct mechanical deflection of the cupula or hair cell bundle is necessary. This has been instrumental in studying the auditory and vestibular system in amphibians (Corey and Hudspeth 1983; Keen and Hudspeth 2006). Our experimental preparation allows us, for the first time, to carefully stimulate the lateral line system with high spatial and temporal resolution. This greatly increases our ability to characterize how cupular motion of a single neuromast is encoded in the activity of afferent neurons and leads to a behavioral motor response. Understanding how a single neuromast encodes flow information promises to advance, in a quantitative way, our understanding of the lateral line system.

ACKNOWLEDGMENTS

We thank Rafael Levi and Masashige Taguchi for comments on the manuscript and Maxine Floyd and Melissa Ard for excellent fish care.

GRANTS

This work was supported by a postdoctoral fellowship from the Deutsche Forschungsgemeinschaft (HA 6481/1-1) to M. Haehnel-Taguchi and National Institute on Deafness and Other Communications Disorders Grant RO1-DC-010809 and National Science Foundation Grant IOS 1257150 to J. C. Liao.

DISCLOSURES

No conflicts of interest, financial or otherwise, are declared by the author(s).

AUTHOR CONTRIBUTIONS

Author contributions: M.H.-T. and J.C.L. conception and design of research; M.H.-T. performed experiments; M.H.-T. and O.A. analyzed data; M.H.-T., O.A., and J.C.L. interpreted results of experiments; M.H.-T. and O.A. prepared figures; M.H.-T., O.A., and J.C.L. drafted manuscript; M.H.-T., O.A., and J.C.L. edited and revised manuscript; M.H.-T., O.A., and J.C.L. approved final version of manuscript.

REFERENCES

Brand M, Granato M, Nüsslein-Volhard C. Keeping and raising zebrafish. In: *Zebrafish: Practical Approach*. New York: Oxford University Press, 2000, p. 7–37.

Budick SA, O'Malley DM. Locomotor repertoire of the larval zebrafish: swimming, turning and prey capture. *J Exp Biol* 203: 2565–2579, 2000.

Chagnaud BP, Brucker C, Hofmann MH, Bleckmann H. Measuring flow velocity and flow direction by spatial and temporal analysis of flow fluctuations. *J Neurosci* 28: 4479–4487, 2008.

Coombes S, Conley RA. Dipole source localization by mottled sculpin. I. Approach strategies. *J Comp Physiol A* 180: 387–399, 1997.

Coombs S, Janssen J. Peripheral processing by the lateral line system of the mottled sculpin (*Cottus bairdi*). In: The Mechanosensory Lateral Line, edited by Coombs S, Görner P, and Münz H. New York: Springer, 1989, p. 299–319.

Corey DP, Hudspeth AJ. Kinetics of the receptor current in bullfrog saccular hair cells. *J Neurosci* 3: 962–976, 1983.

Denton EJ, Gray J. Mechanical factors in the excitation of clupeid lateral lines. *Proc R Soc Lond B Biol Sci* 218: 1–26, 1983.

Dijkgraaf S. The functioning and significance of the lateral-line organs. *Biol Rev Camb Philos Soc* 38: 51–105, 1963.

Douglass AD, Kraves S, Deisseroth K, Schier AF, Engert F. Escape behavior elicited by single channel rhodopsin-2-evoked spikes in zebrafish somatosensory neurons. *Curr Biol* 18: 1133–1137, 2008.

Engelmann J, Hanke W, Mogdans J, Bleckmann H. Hydrodynamic stimuli and the fish lateral line. *Nature* 408: 51–52, 2000.

Fero K, Yokogawa T, Burgess HA. The behavioral repertoire of larval zebrafish. In: *Zebrafish Model in Neurobehavioral Research*, edited by Kalueff AV and Cachat JM. Clifton, NJ: Humana, 2011, p. 249–291.

Flock A, Wersall J. A study of the orientation of the sensory hairs of the receptor cells in the lateral line organ of fish, with special reference to the function of the receptors. *J Cell Biol* 15: 19–27, 1962.

Goerner P. Untersuchungen zur Morphologie und Elektrophysiologie des Seitenlinienorgans vom Krallenfrosch (*Xenopus laevis Daudin*). *J Comp Physiol A* 47: 316–338, 1963.

Haehnel M, Taguchi M, Liao JC. Heterogeneity and dynamics of lateral line afferent innervation during development in zebrafish (*Danio rerio*). *J Comp Neurol* 520: 1376–1386, 2011.

Haykin SO. *Neural Networks: A Comprehensive Foundation*. Englewood Cliffs, NJ: Pearson Prentice Hall, 1998, p. 842.

Jeffress LA. A place theory of sound localization. *J Comp Physiol Psychol* 41: 35–39, 1948.

Jielof R, Spoor A, de Vries H. The microphonic activity of the lateral line. *J Physiol* 116: 137–157, 1952.

Keen EC, Hudspeth AJ. Transfer characteristics of the hair cell's afferent synapse. *Proc Natl Acad Sci U S A* 103: 5537–5542, 2006.

Kohashi T, Nakata N, Oda Y. Effective sensory modality activation an escape triggering neuro switches during early development in zebrafish. *J Neurosci* 32: 5810–5820, 2012.

Kroese ABA, Schellart NAM. Velocity- and acceleration-sensitive units in the trunk lateral line of the trout. *J Neurophysiol* 68: 2212–2221, 1992.

Liao JC. Organization and physiology of posterior lateral line afferent neurons in larval zebrafish. *Biol Lett* 6: 402–405, 2010.

Liao JC, Haehnel M. Physiology of afferent neurons in larval zebrafish provides a functional framework for lateral line somatotopy. *J Neurophysiol* 107: 2615–2623, 2012.

Liao JC, Fetcho JR. Shared versus specialized glycinergic spinal interneurons in axial motor circuits of larval zebrafish. *J Neurosci* 28: 12982–12992, 2008.

Liu KS, Fetcho JR. Laser ablations reveal functional relationships of segmental hindbrain neurons in zebrafish. *Neuron* 23: 325–335, 1999.

Liu YC, Bailey I, Hale ME. Alternative startle motor patterns and behaviors in the larval zebrafish (*Danio rerio*). *J Comp Physiol A* 198: 11–24, 2012.

Masino MA, Fetcho JR. Fictive swimming motor patterns in wild type and mutant larval zebrafish. *J Neurophysiol* 93: 3177–3188, 2005.

McHenry MJ, Feitl KE, Strother JA, Van Trump WJ. Larval zebrafish rapidly sense the water flow of a predator's strike. *Biol Lett* 5: 477–479, 2009.

McHenry MJ, Liao JC. The hydrodynamics of flow sensing. In: *The Lateral Line System*, edited by Coombs S, Bleckmann H, Fay RR, and Popper AN. New York: Springer, 2014.

Metcalfe WK, Kimmel CB, Schabtach E. Anatomy of the posterior lateral line system in young larvae of the zebrafish. *J Comp Neurol* 233: 377–389, 1985.

Mogdans J, Bleckman H. Responses of goldfish trunk lateral line to moving objects. *J Comp Physiol A* 182: 659–676, 1998.

Montgomery J, Coombs S. Physiological characterization of lateral line function in the Antarctic fish *Trematomus bernacchii*. *Brain Behav Evol* 40: 209–216, 1992.

Montgomery JC, Baker CF, Carton AG. The lateral line can mediate rheotaxis in fish. *Nature* 389: 960–963, 1997.

Müller UK, van Leeuwen JL. Swimming of larval zebrafish: ontogeny of body waves and implications for locomotory development. *J Exp Biol* 207: 853–868, 2004.

Nagiel A, Andor-Ardó D, Hudspeth AJ. Specificity of afferent synapses onto plane-polarized hair cells in the posterior lateral line of the zebrafish. *J Neurosci* 28: 8442–8453, 2008.

Olszewski J, Haehnel M, Taguchi M, Liao JC. Zebrafish larvae exhibit rheotaxis and can escape a continuous suction source using their lateral line. *PLos One* 7: e36661, 2012.

Ricci AJ, Bai JP, Song L, Lv C, Zenisek D, Santos-Sacchi J. Patch-clamp recordings from lateral line neuromast hair cells of the living zebrafish. *J Neurosci* 33: 3131–3134, 2013.

Rosenblatt F. The perceptron: a probablistic model for information storage and organization in the brain. *Psychol Rev* 65: 386–408, 1958.

Sand A. The mechanism of the lateral sense organs of fishes. *Proc R Soc Lond B Biol Sci* 123: 472–495, 1937.

Schulze FE. Ueber die Sinnesorgane der Seitenlinie bei Fischen und Amphibien. *Archiv Mikroskopische Anatomie* 6: 62–88, 1870.

Trapani JG, Nicolson T. Mechanism of spontaneous activity in afferent neurons of the zebrafish lateral-line organ. *J Neurosci* 31: 1614–1623, 2011.

van Netten SM. Hydrodynamic detection by cupulae in a lateral line canal: functional relations between physics and physiology. *Biol Cybern* 94: 67–85, 2006.

van Netten SM. Laser interferometric measurements on the dynamic behaviour of the copula in the fish lateral line. *Hear Res* 29: 55–61, 1987.

Voigt R, Carton AG, Montgomery JC. Responses of anterior lateral line afferent neurones to water flow. *J Exp Biol* 203: 2495–2502, 2000.